

# Modeling of the Sputtering Efficiency for Martian Atmosphere

Y.-C. Wang<sup>1</sup>, J.G. Luhmann<sup>1</sup>, F. Leblanc<sup>2</sup>, X. Fang<sup>3</sup>, R.E. Johnson<sup>4</sup>, Y. Ma<sup>5</sup>, W.-H. Ip<sup>6</sup>, and L. Li<sup>7</sup>

**1.** Space Sciences Laboratory, University of California at Berkeley, 7 Gauss Way, Berkeley, CA94720, USA. **2.** LATMOS/IPSL-CNRS, Université Pierre et Marie Curie, France. **3.** Laboratory for Atmospheric and Space Physics, University of Colorado, 3665 Discovery Drive, Boulder, CO 80303, USA. **4.** Department of Engineering Physics, University of Virginia, Charlottesville, VA22904, USA. **5.** Institute of Geophysics and Planetary Physics, University of California, Los Angeles, California, USA. **6.** Institute of Astronomy and Space Science, National Central University, No. 300, Jhongda Rd, Jhongli City, Taoyuan County 32001, Taiwan, ROC. **7.** State Key Laboratory of Space Weather, Center for Space Science and Applied Research, Chinese Academy of Sciences, Beijing, China.

E-mail address: jinnee.ycwang@ssl.berkeley.edu (Y.-C. Wang)

## Abstract

The formation of a hot corona with the related escape rate of the oxygen atoms is an important issue affecting the evolution of the Martian atmosphere. While the dissociative recombination process appears to dominate the non-thermal escaping rate of the oxygen atoms, atmospheric sputtering by the re-impact of the pickup exospheric ions could have played a role in earlier epochs and at solar maximum in the present epoch. Due to the orientation of the interplanetary magnetic fields and the shielding of the crustal fields near Mar's surface, the pickup ions may re-impact the atmosphere with a variety of angles, energies, and spatial distributions. While night-side sputtering is suggested to occur based on modeling (L. Li et al., *JGR* 116, A08204, 2011), the sputter component due to pickup ion impacts on the oxygen corona can be distinguished from other ejection mechanisms, such as dissociative recombination. In preparation for the Maven mission, we performed a Monte Carlo model of the upper atmosphere coupled to a molecular dynamic calculation for the molecular collisions developed by F. Leblanc and R.E. Johnson (*JGR* 107, 5010, 2002) to study the cascade sputtering effects in the region of the Martian exobase. Different incident angle and energy spectrum of the impact ions were tested. Further calculations with more realistic pickup ion impact distributions will be performed based on the numerical results of a 3D Monte Carlo Pickup Ion Transport model, which includes the electromagnetic backgrounds from the 3D multi-species MHD simulations (Y. Ma et al., *JGR* 109, A07211, 2004; Y. Ma and A. F. Nagy, *GRL* 34, L08201, 2007).

## 1. Introduction

- The re-impact of the  $\text{pick-up O}^+$  could have played a role in earlier epochs and at solar maximum in the present epoch (J.G. Luhmann et al., *GRL* 19, 2151-2154, 1992).
- The night-side sputtering can contribute hot corona at anti-sunward hemisphere (L. Li et al., *JGR* 116, A08204, 2011).

## 2. Atmospheric Sputtering Model

- A Monte Carlo model of the upper atmosphere coupled to a molecular dynamic calculation (F. Leblanc and R.E. Johnson, *JGR* 107, 5010, 2002) is used to simulate the pick-up  $\text{O}^+$  sputtering.
- The background atmospheres are shown in Figure 1 (Ma et al., *JGR* 109, A07211, 2004).
- Different incident zenith angles and energies of  $\text{O}^+$  are tested with the sputtering model at fixed location and flux ( $3.12 \times 10^{22} \text{ s}^{-1}$ ). The escaping yields are calculated as

$$\text{Yield} = \frac{\text{Number of Escape Neutrals}}{\text{Number of Incident Ions (Glancing Ions included)}}$$

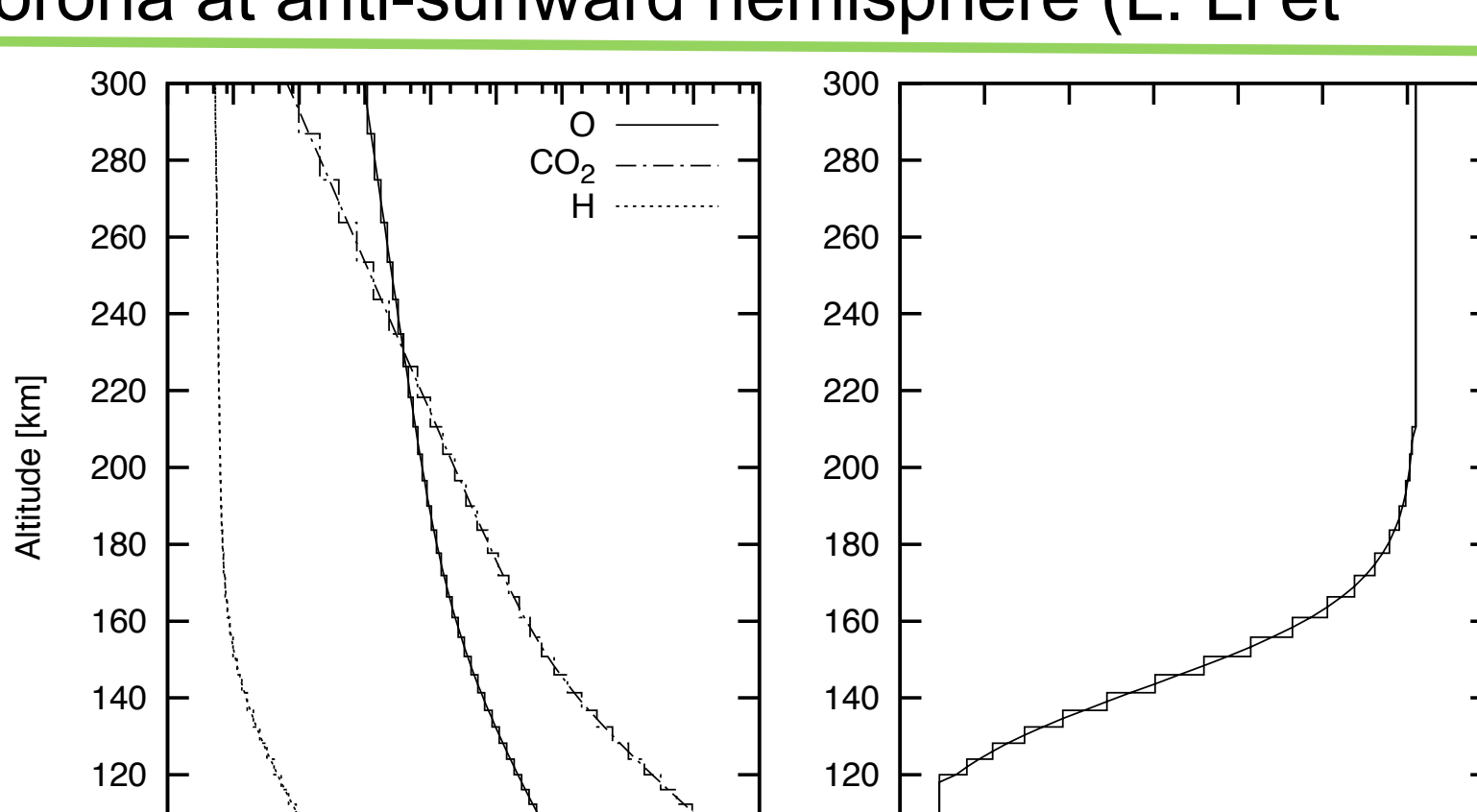


Figure 1. Uniform background atmospheric number densities and temperature distributions (Ma et al., 2004) used in the sputtering model.

## • Pick-up $\text{O}^+$ impact flux

There are four major factors which will influence the incident flux, zenith angles and energies.

- (1) Electric field acceleration/reflection
- (2) Crustal magnetic field shielding
- (3) Low magnetic field region
- (4) Tail recycling

Active case is shown as an example.

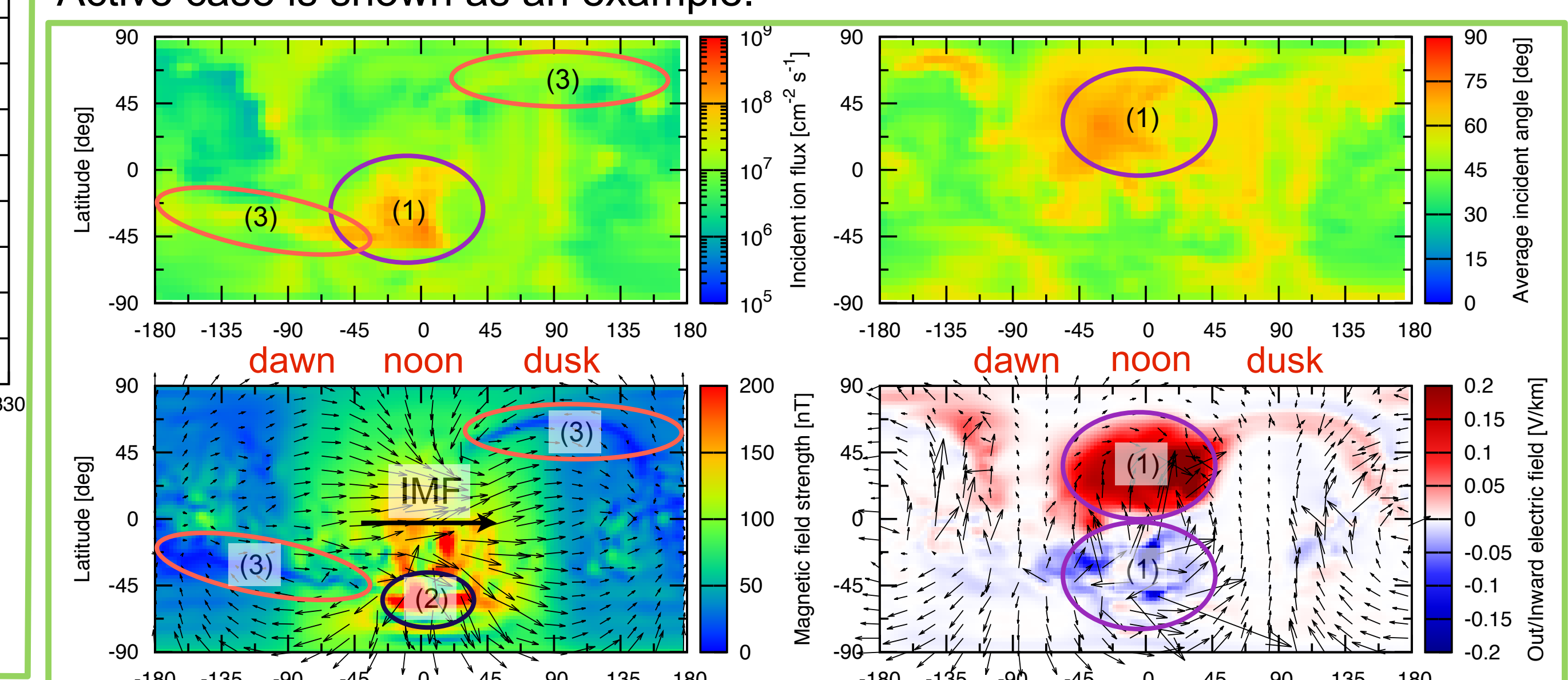


Figure 1. Uniform background atmospheric number densities and temperature distributions (Ma et al., 2004) used in the sputtering model.

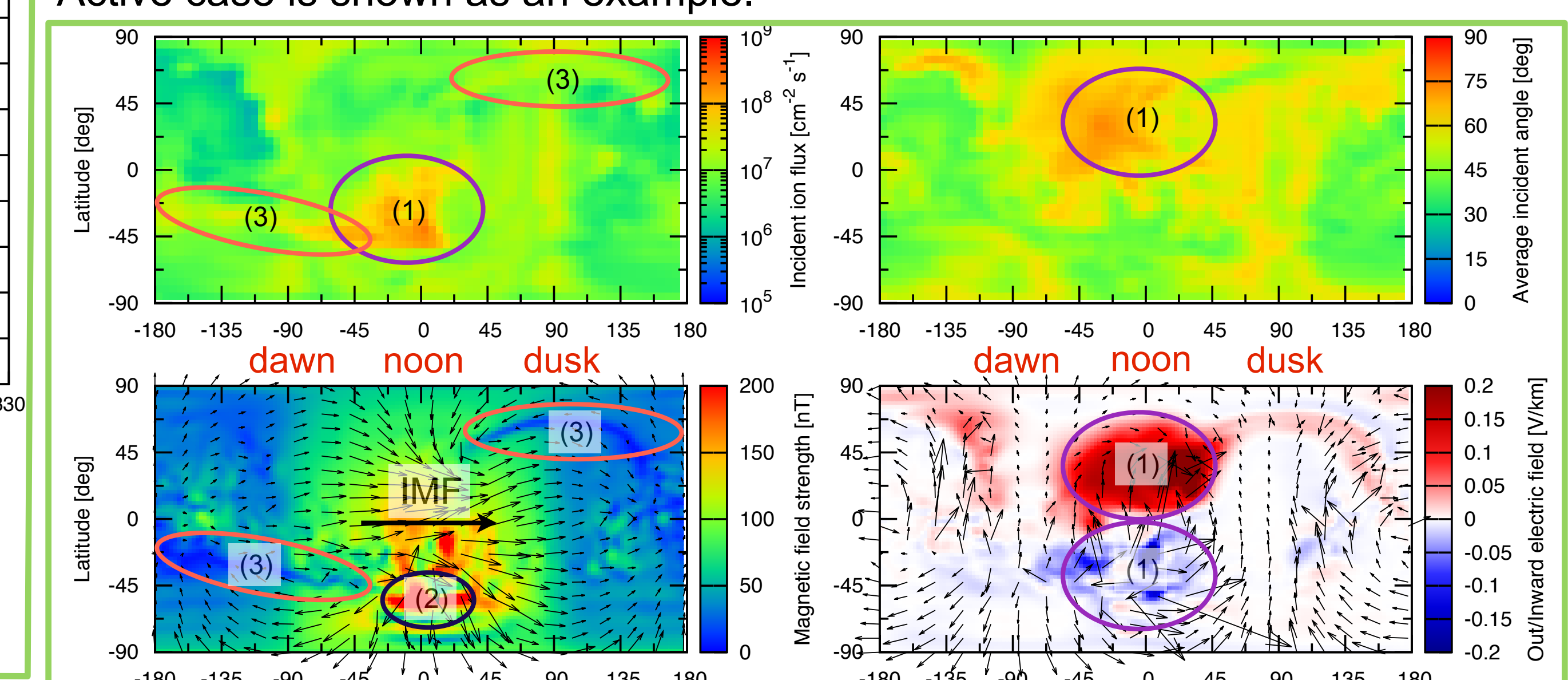


Figure 4. The incident pick-up  $\text{O}^+$  flux and averaged zenith angle distribution for active case are compared with the magnetic and electric field at altitude = 300 km.

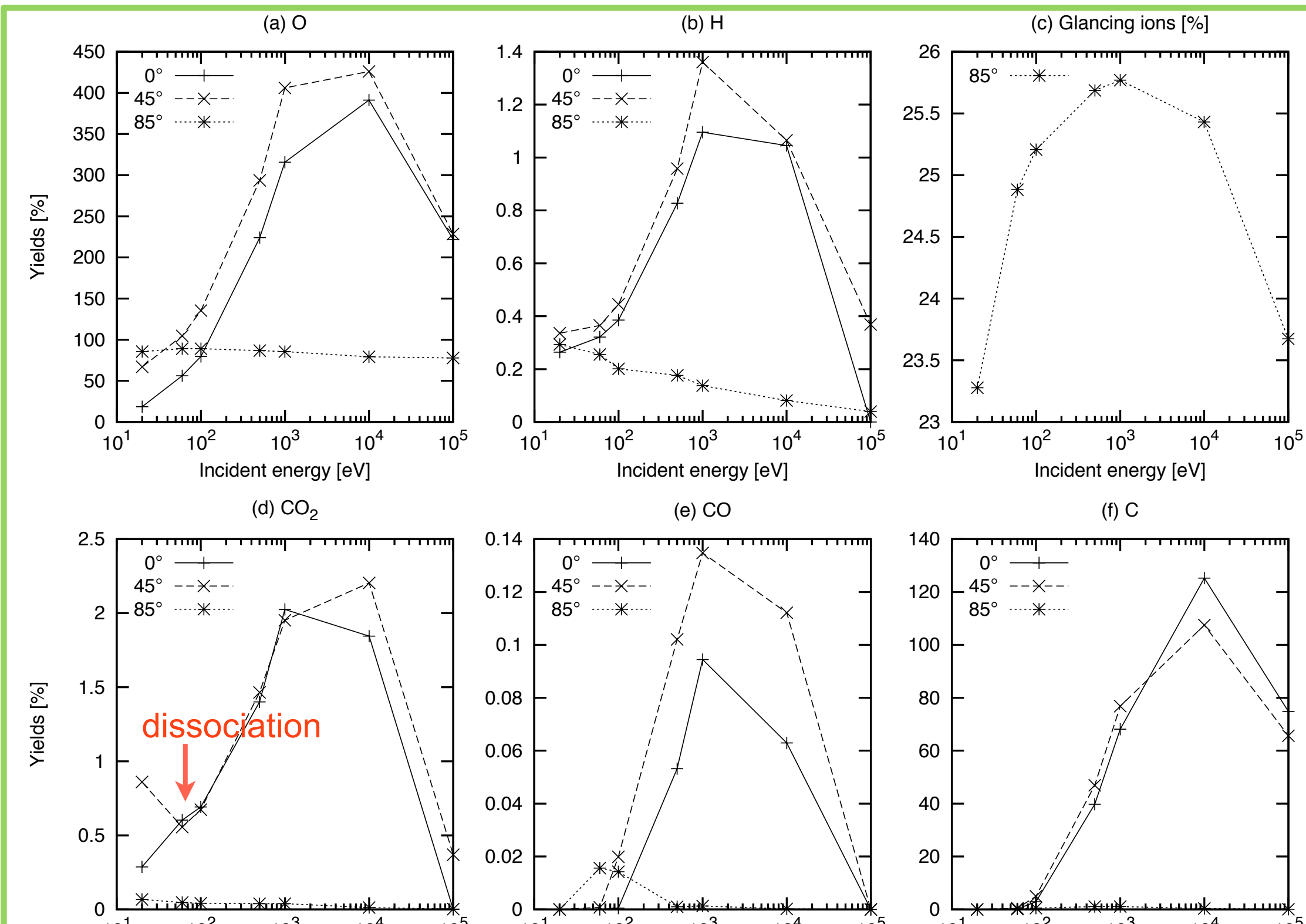
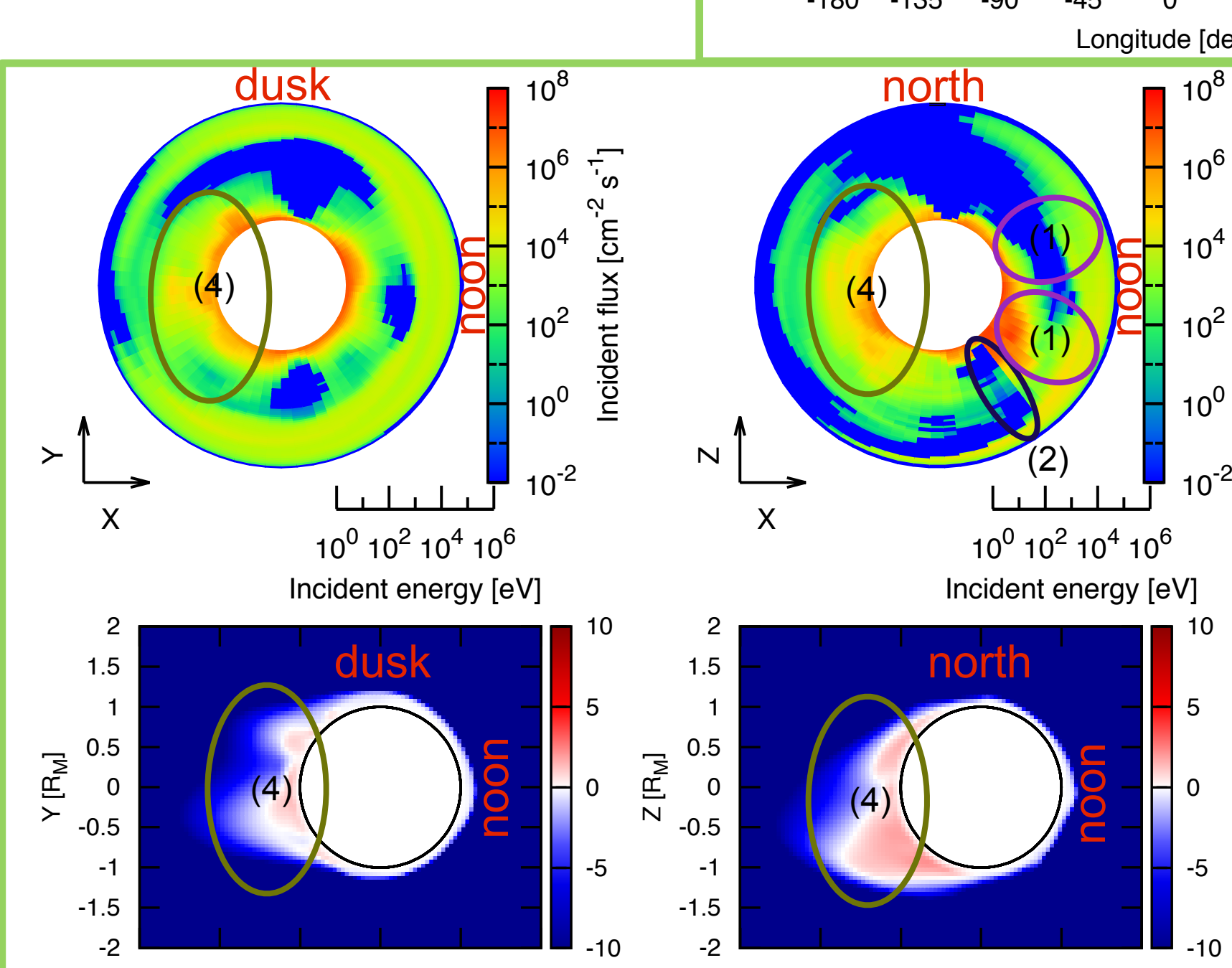


Figure 2. Escaping yields for different incident ion zenith angles and energies.



## • Atmospheric responses

The sputtering yields, hot corona distribution, and influences to the background atmosphere are shown as follows. Randomly distributed and fixed (westward and southward) incident azimuth angle are tested to see their effects on the atmosphere.

Solar activities	Escaping yields	O	$\text{CO}_2$	CO	C	H	Glancing ions
Nominal Quiet Flux = $1.2 \times 10^{25} \text{ s}^{-1}$							
Random azimuth angle	9.5%	0.04%	0.0046%	0.96%	0.19%	0.3%	
Westward azimuth angle	9.02%	0.039%	0.0013%	0.93%	0.23%	0.3%	
Southward azimuth angle	8.5%	0.033%	0.0034%	0.92%	0.22%	0.3%	
Nominal Active Flux = $2.5 \times 10^{25} \text{ s}^{-1}$							
Random azimuth angle	8.6%	0.035%	0.0018%	0.38%	0.23%	0.44%	
Westward azimuth angle	7.5%	0.023%	0.00056%	0.37%	0.24%	0.45%	
Southward azimuth angle	8.2%	0.03%	0.00058%	0.38%	0.23%	0.44%	
Extreme Flux = $8.9 \times 10^{25} \text{ s}^{-1}$							
Random azimuth angle	60.4%	0.3%	0.026%	6.46%	0.26%	0.9%	
Westward azimuth angle	45.2%	0.23%	0.02%	6.6%	0.24%	0.8%	
Southward azimuth angle	56.7%	0.25%	0.04%	6.15%	0.3%	0.9%	

Table 2. Sputtering yields for different cases.

Figure 5. The incident pick-up  $\text{O}^+$  energy distribution in XY, XZ, and YZ planes for active case are show in the upper panel. Relative plasma flow in XY and XZ planes are also shown in the lower panel.

\* The incident energy distribution will have direct correlations to the structure of the sputtered hot corona.

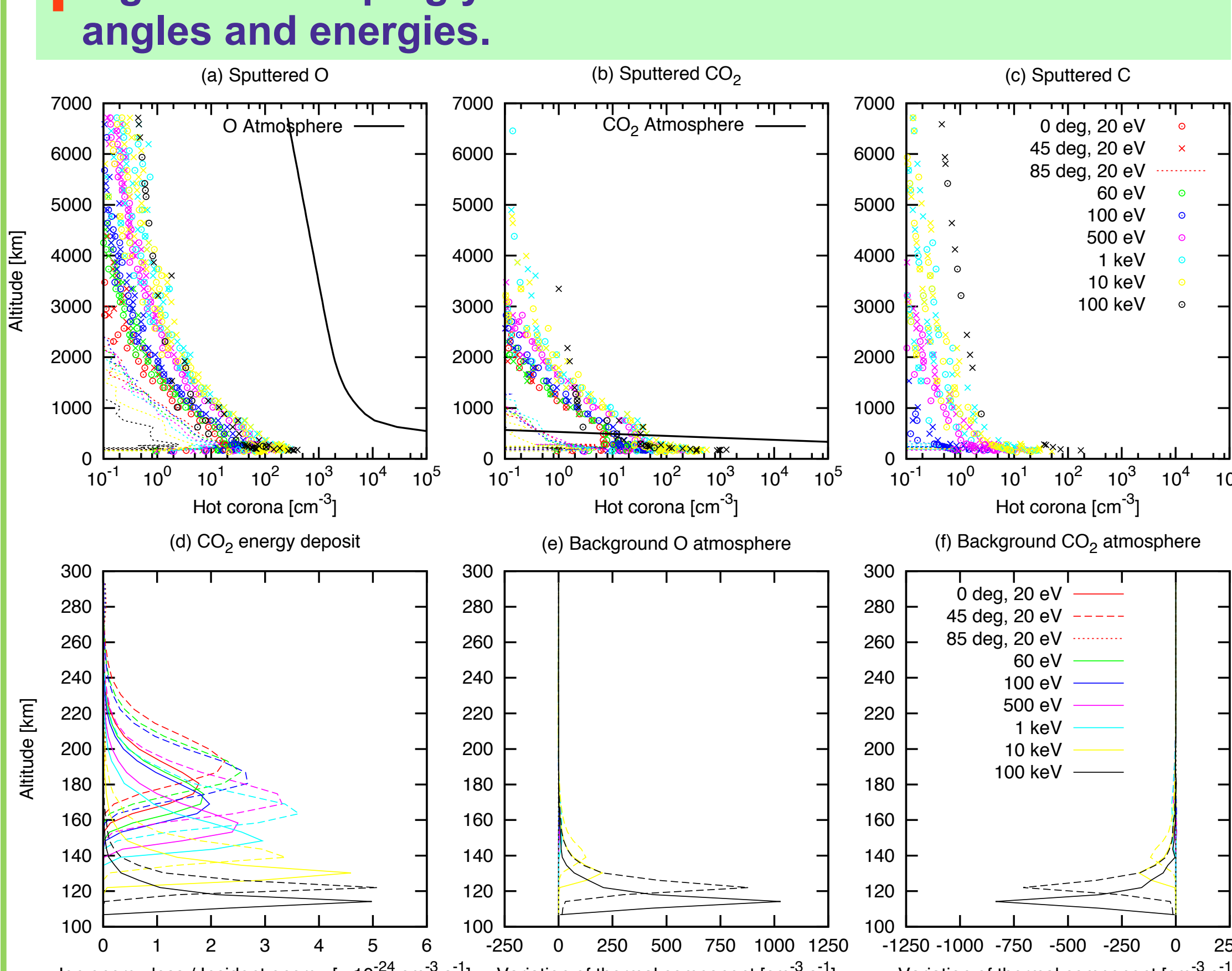


Figure 3. (a)-(c) The sputtered hot corona, (d) ion energy deposit, and (e)-(f) number density variation of the thermal atmospheres for different incident zenith angles and energies.

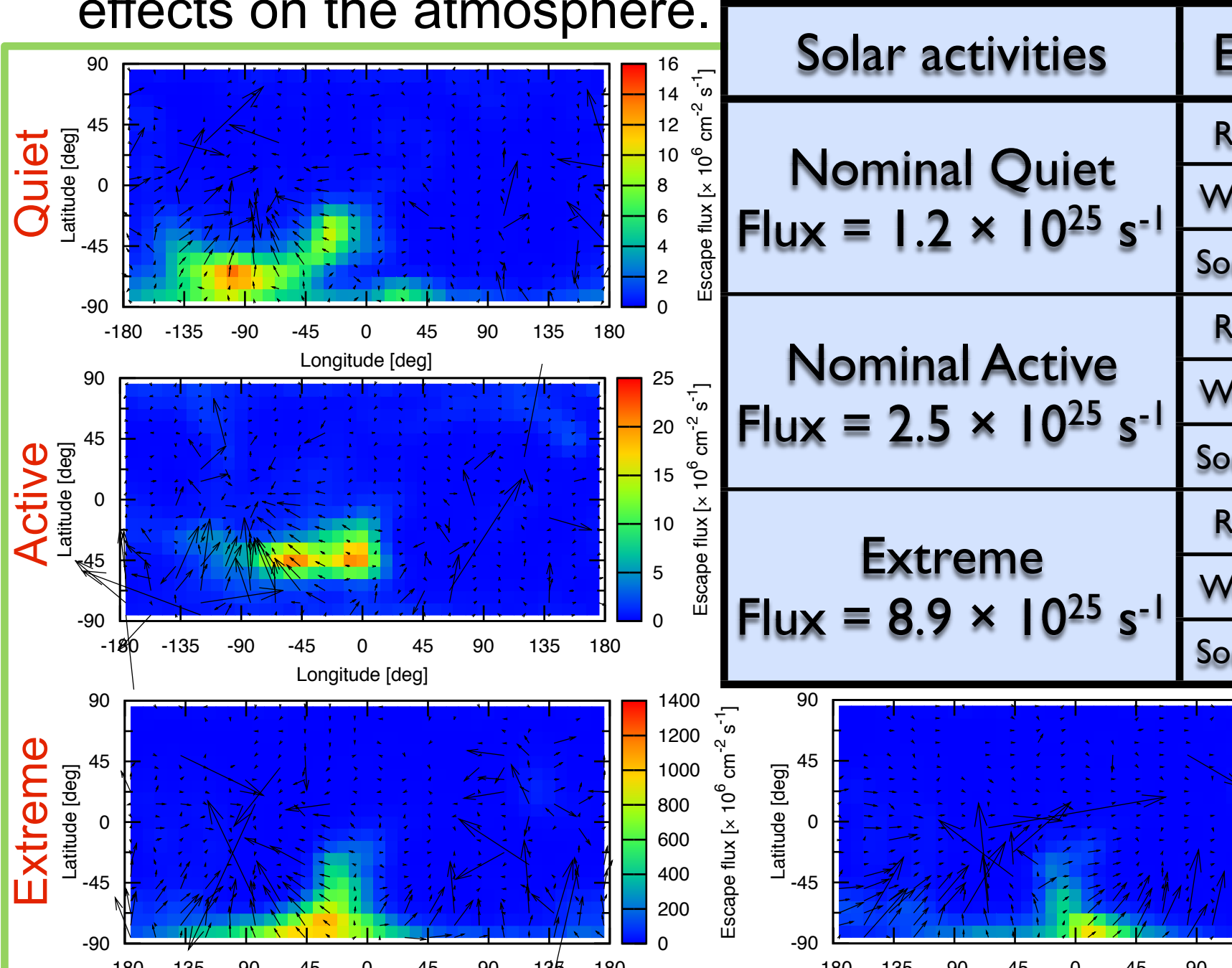


Figure 6. Escape flux distributions for different solar activity cases and incident azimuth angle distributions.

## 3. Responses to realistic $\text{O}^+$ sputtering

- The electromagnetic fields for three different solar activities are simulated with MHD model (Y. Ma et al., *JGR* 109, A07211, 2004; Y. Ma and A. F. Nagy, *GRL* 34, L08201, 2007). The resultant pick-up  $\text{O}^+$  recycling is calculated with Monte Carlo method based on the MHD results (Table 1).

Solar activities	$n_{sw}$	$v_{sw}$	IMF
Nominal Quiet	$4 \text{ cm}^{-3}$	400 km/s	3 nT (56° in XY-plane)
Nominal Active	$4 \text{ cm}^{-3}$	1200 km/s	3 nT (y-component)
Extreme	$20 \text{ cm}^{-3}$	1000 km/s	20 nT (y-component)

Table 1. Three solar activity parameters.

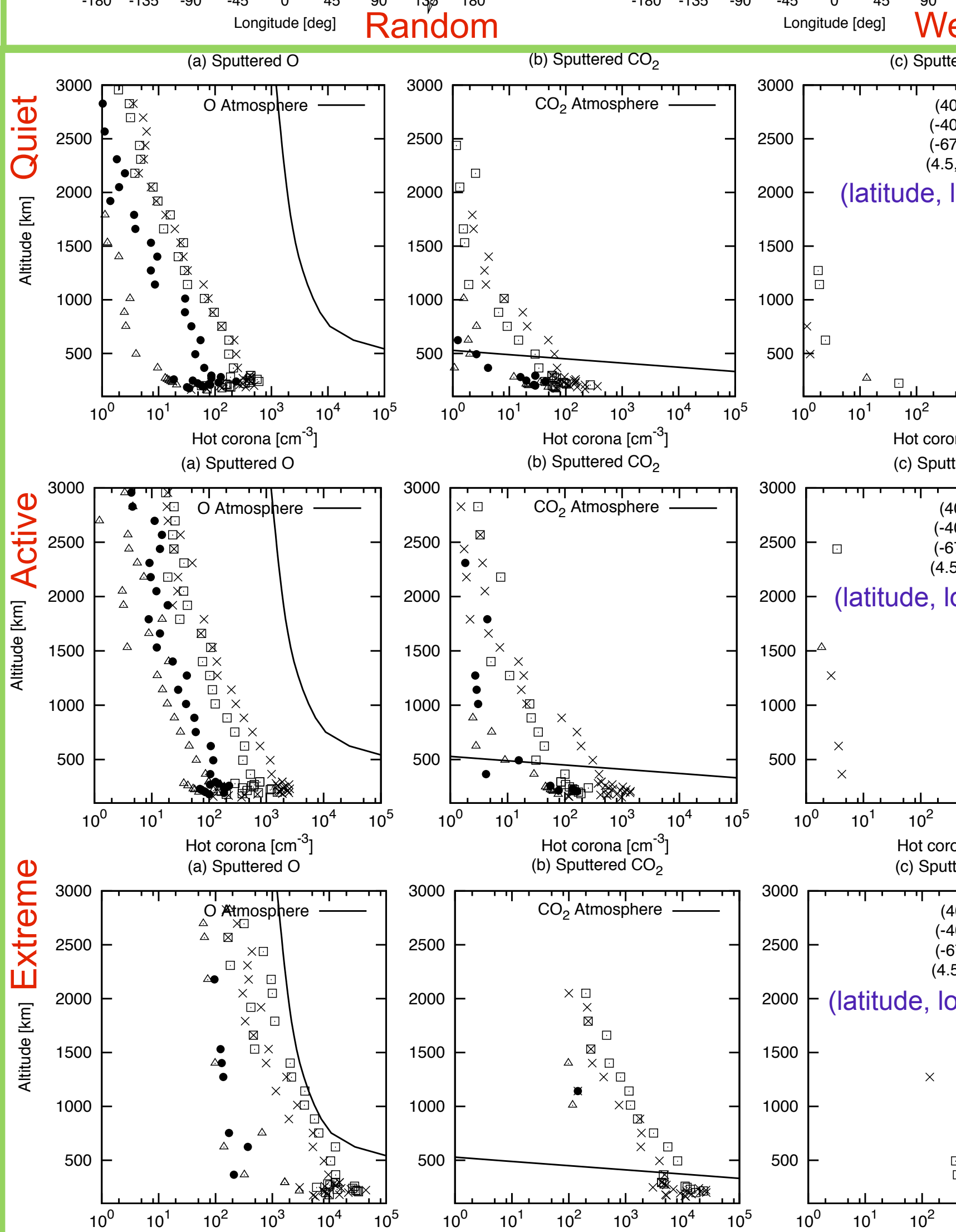
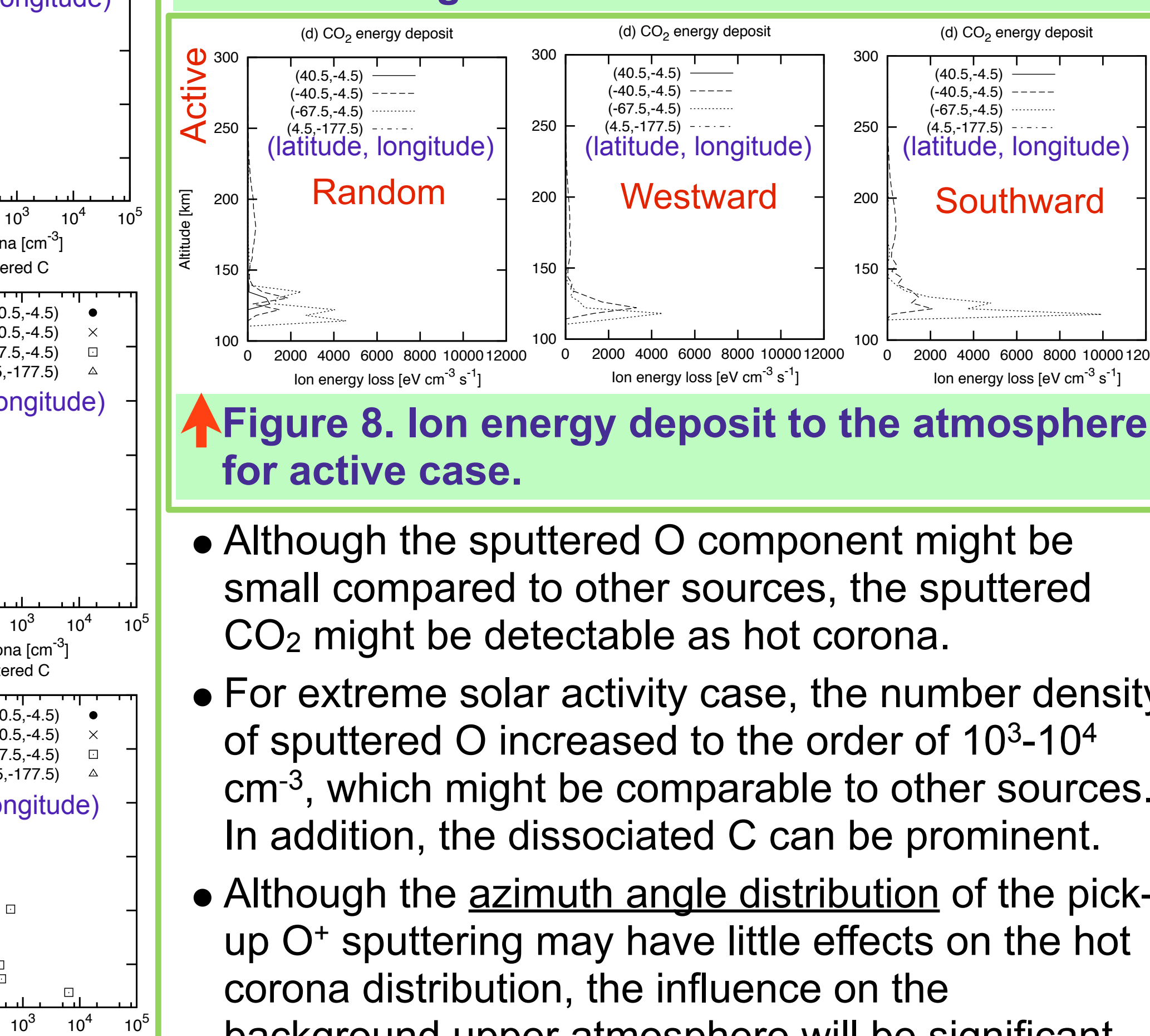


Figure 7. The sputtered hot corona for different solar activity cases with randomly distributed azimuth angle.



- Although the sputtered O component might be small compared to other sources, the sputtered  $\text{CO}_2$  might be detectable as hot corona.
- For extreme solar activity case, the number density of sputtered O increased to the order of  $10^3\text{-}10^4 \text{ cm}^{-3}$ , which might be comparable to other sources. In addition, the dissociated C can be prominent.
- Although the azimuth angle distribution of the pick-up  $\text{O}^+$  sputtering may have little effects on the hot corona distribution, the influence on the background upper atmosphere will be significant.